

Determining the Significance of Electrodynamic Coupling Between Superthermal Electrons and Thermal Plasma

M. W. Liemohn and G. V. Khazanov

Space Sciences Laboratory, NASA Marshall Space Flight Center, ES-83, Huntsville, Alabama

The necessity of electrodynamic coupling in addition to collisional coupling between superthermal electrons (SEs) and thermal plasma is discussed. Collisional coupling typically involves Coulomb collision terms in the SE kinetic equation and heating rate terms in the thermal plasma energy equations. Electrodynamic coupling encompasses the inclusion of superthermal electron terms in the quasineutrality condition, flux balance equation, and electric field formulation, as well as the inclusion of the self-consistent electric field in the SE kinetic equation. The case of plasmaspheric refilling is investigated, and two methods of quantitatively determining when electrodynamic effects are important and should be included in the calculation are presented. Using the methods determined from the previous case, results from a polar wind numerical calculation are investigated and it is determined that even a very small amount of photoelectrons are significant in the polar cap.

INTRODUCTION

Superthermal electrons (SEs) are an important part of near-Earth space plasma, often traveling vast distances before depositing their energy through various mechanisms. The effects of SEs on the thermal plasma can be significant, sometimes even the dominant process in the formation of the thermal plasma distribution, and so it is often necessary to include these effects in thermal plasma calculations.

The influence of superthermal electrons has been known for many decades beginning with studies of ionospheric temperatures [e.g., *Hanson*, 1963]. These effects were determined to be caused by both local SE production [*Hoegy et al.*, 1965] and by nonlocal production, specifically from the conjugate ionosphere [*Fontheim et al.*, 1968]. *Nagy and Banks* [1970] developed the first two-stream kinetic model of SE transport in the ionosphere, and many other SE transport models soon followed [Cf. the review sections of *Cicerone et al.*, 1973; *Winningham et al.*, 1989; *Khazanov and Liemohn*, 1995]. These models have been used for many purposes, most notably to calculate heating rates into the thermal plasma and excitation rates for atmospheric emissions.

There have been several models that combine the superthermal calculation with that of the thermal plasma. The earliest is *Lemaire* [1972], who developed a self-consistent collisionless kinetic description of the polar wind that included a SE population. More recently, the model of *Min et al.* [1993] calculates $E_{||}$ from the thermal plasma equations and then uses this electric field in the steady-state kinetic equation for the superthermal electrons in the aurora and at midlatitudes. *Tam et al.* [1995] treat the ions and superthermal electrons kinetically along with a fluid approach for the thermal electrons, and obtain steady-state

polar wind results that are collisionally and electro-dynamically self-consistent. *Khazanov et al.* [1997] reexamined the collisionless kinetic description of the polar wind to determine the maximum influence of photoelectrons on ion outflows. The first time-dependent model of self-consistent coupling is that of *Liemohn et al.* [1997], where SE effects on thermal plasma refilling were investigated.

In *Liemohn et al.* [1997], a driver program was introduced to couple the time-dependent, spatially-unified, kinetic model of SE transport [*Khazanov and Liemohn, 1995; Liemohn and Khazanov, 1995*] with the time-dependent, field-aligned, hydrodynamic model of the thermal plasma [*Guiter et al., 1995*]. This study self-consistently coupled the two models, both collisionally and electro-dynamically. Collisional coupling involves Coulomb collision terms in the SE kinetic equation and heating rate terms in the thermal plasma energy equations. Electrodynamic (collisionless) coupling encompasses the inclusion of superthermal electron terms in the quasineutrality condition, flux balance equation, and electric field formulation, as well as the inclusion of the self-consistent electric field in the SE kinetic equation. In that study, both of these coupling mechanisms were included all of the time, but the computational cost of electro-dynamically coupling the models is high, and the question should be asked: when is it necessary to electro-dynamically couple the SE and thermal plasma calculations?

This study presents a quantitative method of determining when electrodynamic effects are significant and should be included in the calculation. This analysis is based on results from *Liemohn et al.* [1997], which focused on plasma flows along closed field lines. A case study of results from *Khazanov et al.* [1997] is also conducted, to determine the necessity of self-consistent coupling in the polar cap region in the presence of photoelectrons.

RESULTS

In *Liemohn et al.* [1997], it was determined that the primary electrodynamic coupling mechanism is the inclusion of a SE term in the flux balance equation,

$$\sum_i n_i u_i - n_e u_e - n_s u_s = \frac{j}{e} \quad (1)$$

where the subscripts e , s , and i represent thermal electrons, superthermal electrons, and ion species; n is density; u is bulk flow; and j/e is the current density. This equation was used by setting $j=0$ and solving for the thermal electron flux, with the other fluxes calculated from the hydrodynamic (ions) and kinetic (SE) equations. In that study, photoionization was started in the ionospheres connected to a greatly depleted plasmaspheric flux tube ($L=4$), and the flows of superthermal and thermal plasma along the field line were modeled and analyzed. It was seen that, during the first few minutes of refilling, the thermal electron velocity reverses and flows down from the equatorial plane in the plasmasphere into the ionospheres,

exactly opposite to the case when the SE flux is not included in this equation (see Figure 6 of *Liemohn et al.* [1997]). However, by 15 min the thermal electron velocity had returned to its value without electrodynamic coupling for most of the field line, because the SEs from each ionosphere had balanced each other to the point of reducing the SE flux to an insignificant level in the plasmasphere. Only near the ionospheres was there a difference, because the counterflowing SE streams are not balanced and the SE flux is still quite strong.

Because it is the fluxes (nu) that appear in (1), this quantity should be examined during the early stage time period to determine the conditions leading to the strong electrodynamic coupling between the SEs and the thermal plasma. Figure 1 shows these fluxes for the SEs, thermal electrons, and the sum of the thermal ions at various times after beginning the refilling process, with (solid lines) and without (dotted lines) the SE flux included in (1) (as well as other less significant electrodynamical coupling terms). Note that because it is assumed that there is no current, the thermal electron flux is found by subtracting the SE flux from the total ion flux. In Figure 1, the SE fluxes with and without electrodynamic coupling are quite close to each other, but the fluxes without are slightly bigger. This is because the electric field in the SE kinetic equation decelerates the electrons as they move from the ionospheres towards the equatorial plane. At 10 sec, the SEs dominate equation (1), causing the fluid thermal electrons to compensate with a nearly equal but oppositely-directed particle flux. After 1 min, the thermal ions are developing a stronger presence in (1) near the equatorial plane, and so the thermal electron flux is beginning to change from the SE-dominated case. By 3 min, the ions have become a major term in (1), and the thermal electrons have started flowing back towards the equatorial plane for most of the plasmasphere. After 5 min, the thermal electron flow has almost returned to its "no coupling" levels, and by 15 min the contribution of the superthermal flux term in (1) is significant only in small regions near the ionospheres. Notice that the ion fluxes are nearly identical with and without electrodynamic coupling. The reader is referred to *Liemohn et al.* [1997] for further discussion of the simulation.

ANALYSIS

Qualitatively, it appears that the SE flux term is important only for the first few minutes of refilling. How does this translate into a quantitative algorithm for determining when this form of coupling is necessary in the equations?

First, criteria must be established for setting limits on what significant means in terms of influencing the results. Two possibilities will be discussed: one based on the maximum ratio of SE flux to total ion flux; and another based on the average ratio at any point along the simulation range. For this analysis, the results along the field above $1 R_E$ from the surface in each of the conjugate ionospheres will be used. This is because the plasmasphere is

the region of interest, and so attention will be restricted to the SE contribution in this region.

Method 1: Maximum ratio

The ratio of SE flux to the total ion flux at any point along the field line is given by

$$R(s) = \frac{|n_s(s)u_s(s)|}{\left| \sum_i n_i(s)u_i(s) \right|} \quad (2)$$

and represents the relative contribution of each of these terms to (1). A value greater than unity means that SEs are dominant at this spatial point, while a value less than unity means that the ion flux is dominant. So, one indication that the SE flux is no longer a critical factor in (1) would be to define a threshold value for including or omitting the SE terms. What is needed, then, is the maximum value of this ratio, $R_{\max} = \max[R(s), s=s_{\text{low}} \dots s_{\text{high}}]$, where s_{low} and s_{high} are the limits of the simulation range or the region of interest.

As was mentioned above, though, the SEs were decelerated due to the ambipolar electric field, and so the ratio will be smaller with coupling than without coupling. It is necessary, then, to have two thresholds, one for turning on electrodynamic coupling and the other for turning it off, with some overlap in the values so the processes are not flickering on and off when the results are near the threshold. The following thresholds are proposed: turn this extra coupling on when R_{\max} exceeds 1.0, and turn it off when it falls below 0.5.

Figure 2a shows R_{\max} for the results with and without electrodynamic coupling from Figure 1. The times presented are minutes after the sources are turned on in the ionospheres, as in Figure 1, and are shown out to 30 min of simulation time. Using the above-mentioned thresholds, electrodynamic coupling is important for the first 11 min of refilling, after which time its influence is minimal. The terms would not need to be included during the times shown, because R_{\max} at 30 min without coupling is only 0.7. It should be noted that the results beyond 30 min are reaching the limits of validity for the hydrodynamic model, when unphysical shocks develop and taint the results.

Method 2: Average ratio

Another method of determining the significance of the electrodynamic coupling terms is to use the average ratio of SE flux to total ion flux. The average value for R is defined as

$$R_{\text{av}} = \frac{\int_{s_{\text{low}}}^{s_{\text{high}}} R(s) ds}{\int_{s_{\text{low}}}^{s_{\text{high}}} ds} \quad (3)$$

As with Method 1, two thresholds for R_{av} need to be defined, one for turning coupling on (compared to R_{av} without coupling) and one for turning coupling off

(compared to R_{av} with coupling). These thresholds should be much tighter than those for Method 1, because R_{av} is a measure of the overall influence on the electrodynamic coupling terms. Therefore, turn on and turn off thresholds for R_{av} of 0.10 and 0.05, respectively, will be chosen.

Figure 2b presents R_{av} with and without electrodynamic coupling. As you can see, R_{av} is quite high for the first few minutes of refilling, confirming that the SEs are indeed the major term (1) and that electrodynamic coupling should be included. However, after 11 min, R_{av} drops below 0.05, and the electrodynamic coupling terms no longer have a strong influence on the thermal plasma calculation. Again, R_{av} in Figure 2b does not exceed the turn on threshold, and the influence remains small.

CASE STUDY

It is possible to apply these methods to other cases in order to determine the significance of electrodynamic coupling between superthermal electrons and the thermal plasma. One region of interest is the dayside polar cap, where photoelectrons are thought to play a role in the escape of upflowing ions. At high latitudes, the flows are not balanced by particles streaming down the field line from the conjugate ionosphere, because these field lines are either open or so long that the conjugate point is unimportant. Therefore, the influence of the superthermal electrons in this region should be greater than that at midlatitudes, as was the case for the plasmaspheric refilling study above.

Let us examine the results of *Khazanov et al.* [1997], who presented a collisionless, steady-state kinetic model of the polar wind in the presence of photoelectrons. Their simulation domain is from 500 km out to 5 R_E along a high-latitude, open field line. Examining the Plates in this paper reveals that the photoelectrons have quite an influence on the outflowing ions and thermal electrons, especially for a photoelectron concentration at the base greater than 0.1%. Let us examine these results based on the analysis above.

The flux calculation in *Khazanov et al.* [1997] for the kinetic populations is given by

$$n_{\alpha}(s)u_{\alpha}(s) = n_{0\alpha}u_{0\alpha} \left[1 - y_{s^{ub}}^2 \exp \left(- \frac{B_{s^{ub}}}{B_0} \frac{z_{\alpha}(s^{ub})}{y_{s^{ub}}^2} \right) \right] \quad (4)$$

$$\times \frac{B(s)}{B_{s^{ub}}} e^{-z_{\alpha}(s^{ub})} = \frac{B(s)}{B_{s^{ub}}} n_{\alpha}(s^{ub})u_{\alpha}(s^{ub})$$

Here $z_{\alpha}(s)$ depends on the difference of the electrostatic and gravitational potentials, y is a function of the magnetic field strength $B(s)$, the "0" subscript refers to the boundary conditions at the base altitude, and s^{ub} is the upper level of the simulation domain. This shows that the fluxes of photoelectrons, oxygen ions, and hydrogen ions are only dependent on the flux at s^{ub} and the magnetic field strength. Therefore, $R(s)$ from (2) will be constant and

R_{\max} will be equal to R_{av} . In this case, the thresholds for turning on and off electrodynamic coupling should be taken from method 2 above.

Results from this study are presented in Figure 3. It should be noted that the boundary conditions (at $500 R_E$) are $6 \times 10^4 \text{ cm}^{-3}$ for O^+ , $1 \times 10^3 \text{ cm}^{-3}$ for H^+ , ion temperatures of 2000 K, a thermal electron temperature of 2500 K, and a 20 eV characteristic energy for the photoelectrons. The fluxes at the upper boundary ($5 R_E$) for the three populations are given in Figure 3a. Notice that the proton fluxes are unaffected by the presence of photoelectrons in these results. This is because the protons are escaping along the field line even when there are no photoelectrons, and thus the flux of these particles is determined entirely by the boundary condition at the base. The oxygen ion fluxes, however, are greatly dependent on the photoelectrons, and even surpass the proton flux for $n_{pe} \geq 0.5\%$.

The flux ratio is shown in Figure 3b. The curve has reached an asymptote from roughly $n_{pe} \sim 0.1\%$ and below. The curvature of the result at the upper end of the scale indicates that there could be another high concentration asymptotic limit. The ratio crosses unity near $n_{pe} = 0.003\%$, and the trend towards $R=0$ as n_{pe} goes to zero is seen. Because these results are all produced with electrodynamic coupling included, the turn-off threshold is $R=0.05$, which is the case for $n_{pe} \leq 0.0002\%$. This is a very small concentration of photoelectrons.

Another indicator of superthermal-thermal plasma coupling is the oxygen density profile, plotted in Figure 4. Results are shown up to 4000 km, below which the distributions for widely different photoelectron contents are similar enough to show on the same scale. Notice that the change in the O^+ density is getting bigger with increasing photoelectron concentration. This is also seen in the O^+ flux at $5 R_E$ presented in Figure 3. At low n_{pe} values, oxygen has little response, then it goes through a rapid response with a maximum near $n_{pe} = 0.05\%$, and then begins to asymptote again at very high photoelectron concentrations.

The electrodynamic coupling between photoelectrons and the thermal plasma in the polar cap region was originally discussed by *Lemaire* [1972]. Using the collisionless, steady-state kinetic equation for all species (H^+ , O^+ , thermal electrons, and photoelectrons), he also showed increased ion densities at high altitudes when photoelectrons were included. It is therefore useful to show a comparison of his results with results from the *Khazanov et al.* [1997] model for similar boundary conditions. The boundary conditions, taken at a low altitude limit of 950 km, are $7 \times 10^3 \text{ cm}^{-3}$ for O^+ , 320 cm^{-3} for H^+ , thermal plasma species temperatures of 3000 K, and a 10 eV photoelectron characteristic energy. It is expected that the lower densities and higher temperatures for the thermal plasma, combined with a lower characteristic energy for the photoelectrons, should decrease the photoelectron influence from that calculated above.

A comparison of the results of *Lemaire* [1972] with that of *Khazanov et al.* [1997] is shown in Figure 5. Both models predict that n_{H^+} is not affected by the presence of photoelectrons at the concentrations taken for these calculations (0.0% and 0.0094% at 950 km). Also, both models predict a crossover of the O^+ and H^+ densities at an altitude of less than an R_E . The O^+ densities increase very slightly with the inclusion of the photoelectrons. This concentration of 0.0094% is quite low, so it is not surprising that the influence is small, similar to Figure 4. In Figure 4, however, the influence at $n_{p0}=0.01\%$ is greater than the influence here in Figure 5, as expected from the differing boundary conditions. For $n_{p0}=0.0094\%$, $R=0.439$, indicating these results are close to $n_{p0}\sim 0.002\%$ in the case study above. However, the thermal electron fluxes are still influenced by the presence of the photoelectrons, and inclusion of self-consistent electrodynamic coupling is advised. A similar situation arose in the plasmaspheric refilling results, where huge changes in the thermal electron distribution were seen without a strong signature in the ion results. Larger changes in the ion results would be expected for $n_{p0}>0.1\%$, as seen in the results of *Khazanov et al.* [1997].

CONCLUSION

Based on the need for fast yet accurate calculations of superthermal and thermal plasma populations, a system of determining when it is necessary to include electrodynamic (collisionless) coupling terms in addition to collisional coupling terms has been presented. Two methods of determining the level of significance the superthermal electron flux has in the flux balance equation are discussed, and, for the plasmaspheric refilling study of *Liemohn et al.* [1997], it was concluded that electrodynamic coupling terms were significant only for the first 11 minutes of the calculation (determined, coincidentally, by both methods). For a case study of the polar wind results of *Khazanov et al.* [1997], it was determined that the self-consistent coupling is unimportant when the photoelectron concentration at the base (500 km) is below 0.0002% of the total plasma density. This very small threshold density indicates that self-consistent coupling should always be taken into account on the dayside polar cap where the upflowing particles are not balanced by flows from the conjugate hemisphere. This conclusion is supported by a comparison with the original photoelectron-polar wind results of *Lemaire* [1972].

Acknowledgments. MWL would like to thank the conveners of the Huntsville96 Workshop for travel support to attend the meeting. This work was supported at the University of Michigan by NASA GSRP grant NGT-51335. MWL held a National Research Council-Marshall Space Flight Center Postdoctoral Research Associateship while this work was performed. GVK was funded at the University of Alabama in Huntsville by the National Science Foundation under grant ATM-9523699, and also held a National Research Council-Marshall Space Flight Center Senior Research Associateship during part of this work.

REFERENCES

- Cicerone, R. J., W. E. Swartz, R. S. Stolarski, A. F. Nagy, and J. S. Nisbet, Thermalization and transport of photoelectrons: A comparison of theoretical approaches, *J. Geophys. Res.*, **78**, 6709, 1973.
- Fontheim, E. G., A. E. Beutler, and A. F. Nagy, Theoretical calculations of the conjugate predawn effects, *Ann. Geophys.*, **24**, 489, 1968.
- Guter, S. M., T. I. Gombosi, and C. E. Rasmussen, Two-stream modeling of plasmaspheric refilling, *J. Geophys. Res.*, **100**, 9519, 1995.
- Hanson, W. B., Electron temperatures in the upper atmosphere, *Space Res.*, **3**, 282, 1963.
- Hoegy, W. R., J.-P. Fournier, and E. G. Fontheim, Photoelectron energy distribution in the F region, *J. Geophys. Res.*, **70**, 5464, 1965.
- Khazanov, G. V., and M. W. Liemohn, Non-steady-state ionosphere-plasmasphere coupling of superthermal electrons, *J. Geophys. Res.*, **100**, 9669, 1995.
- Khazanov G. V., M. W. Liemohn, and T. E. Moore, Photoelectron effects on the self-consistent potential in the collisionless polar wind, *J. Geophys. Res.*, **102**, 7509, 1997.
- Lemaire, J., Effect of escaping photoelectrons in a polar exospheric model, *Space Res.*, **12**, 1413, 1972.
- Liemohn, M. W. and G. V. Khazanov, Non-steady-state coupling processes in superthermal electron transport, in *Cross-Scale Coupling in Space Plasmas, Geophysical Monograph 93*, AGU, 181, 1995.
- Liemohn, M. W., G. V. Khazanov, T. E. Moore, and S. M. Guter, Self-consistent superthermal electron effects on plasmaspheric refilling, *J. Geophys. Res.*, **102**, 7523, 1997.
- Min, Q.-L., D. Lummerzheim, M. H. Rees, and K. Stamnes, Effects of a parallel electric field and the geomagnetic field in the topside ionosphere on auroral and photoelectron energy distributions, *J. Geophys. Res.*, **98**, 19223, 1993.
- Nagy, A. F., and P. M. Banks, Photoelectron fluxes in the ionosphere, *J. Geophys. Res.*, **75**, 6260, 1970.
- Tam, S. W. Y., F. J. Yasseen, T. Chang, and S. B. Ganguli, Self-consistent kinetic photoelectron effects on the polar wind, *Geophys. Res. Lett.*, **22**, 2107, 1995a.
- Winningham, J. D., D. T. Decker, J. U. Kozyra, J. R. Jasperse, and A. F. Nagy, Energetic (>60 eV) atmospheric photoelectrons, *J. Geophys. Res.*, **94**, 15,335, 1989.

G. V. Khazanov and M. W. Liemohn: Space Sciences Laboratory, NASA/MSFC ES-83, Huntsville, AL 35812.

G. V. Khazanov is also at: Center for Space Physics, Aeronomy, and Astrophysics Research, Department of Physics, The University of Alabama in Huntsville, Huntsville, AL 35899.

LIEMOHN AND KHAZANOV: SIGNIFICANCE OF ELECTRODYNAMIC COUPLING

LIEMOHN AND KHAZANOV: SIGNIFICANCE OF ELECTRODYNAMIC COUPLING

LIEMOHN AND KHAZANOV: SIGNIFICANCE OF ELECTRODYNAMIC COUPLING

LIEMOHN AND KHAZANOV: SIGNIFICANCE OF ELECTRODYNAMIC COUPLING

LIEMOHN AND KHAZANOV: SIGNIFICANCE OF ELECTRODYNAMIC COUPLING

LIEMOHN AND KHAZANOV: SIGNIFICANCE OF ELECTRODYNAMIC COUPLING

LIEMOHN AND KHAZANOV: SIGNIFICANCE OF ELECTRODYNAMIC COUPLING

LIEMOHN AND KHAZANOV: SIGNIFICANCE OF ELECTRODYNAMIC COUPLING

LIEMOHN AND KHAZANOV: SIGNIFICANCE OF ELECTRODYNAMIC COUPLING

Figure 1. Particle fluxes from *Liemohn et al.* [1997] of superthermal electrons (left column), thermal electrons (center column), and the total ion flux (right column) during the early stages of plasmaspheric refilling with (solid lines) and without (dotted lines) electrodynamic coupling effects. Results are along an $L=4$ flux tube, with distances measured from the base of the northern ionosphere in Earth radii.

Figure 2. Flux ration calculations showing (a) R_{max} and (b) R_{av} with electrodynamic coupling (solid lines) and without (dotted lines) based on the simulations from *Liemohn et al.* [1997].

Figure 3. (a) SE, H^+ , and O^+ escape fluxes at $5 R_E$ and (b) the flux ratio $R (=R_{max}=R_{av})$ as a function of photoelectron concentration at the base (500 km) for the polar wind results of *Khazanov et al.* [1997].

Figure 4. Oxygen ion density profiles for several photoelectron concentrations at the base for the polar wind results of *Khazanov et al.* [1997].

Figure 5. Polar wind densities from the *Lemaire* [1972] model and the *Khazanov et al.* [1997] model, with and without a photoelectron population included. Note that the boundary conditions are different than those for Figures 3 and 4.

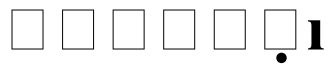
Figure 1. Particle fluxes from *Liemohn et al.* [1997] of superthermal electrons (left column), thermal electrons (center column), and the total ion flux (right column) during the early stages of plasmaspheric refilling with (solid lines) and without (dotted lines) electrodynamic coupling effects. Results are along an $L=4$ flux tube, with distances measured from the base of the northern ionosphere in Earth radii.

Figure 2. Flux ration calculations showing (a) R_{max} and (b) R_{av} with electrodynamic coupling (solid lines) and without (dotted lines) based on the simulations from *Liemohn et al.* [1997].

Figure 3. (a) SE, H^+ , and O^+ escape fluxes at $5 R_E$ and (b) the flux ratio $R (=R_{max}=R_{av})$ as a function of photoelectron concentration at the base (500 km) for the polar wind results of *Khazanov et al.* [1997].

Figure 4. Oxygen ion density profiles for several photoelectron concentrations at the base for the polar wind results of *Khazanov et al.* [1997].

Figure 5. Polar wind densities from the *Lemaire* [1972] model and the *Khazanov et al.* [1997] model, with and without a photoelectron population included. Note that the boundary conditions are different than those for Figures 3 and 4.



File Name : G96EDC.ps

Title : Graphics produced by IDL

Creator : IDL Version 4.0.1 (MacOS PowerMac)

CreationDate : Tue Jul 29 16:10:55 1997

Pages : 1



File Name : Tables1_2.ps

Title : Graphics produced by IDL

Creator : IDL Version 4.0.1 (MacOS Po

CreationDate : Tue Jul 29 15:55:08 19

Pages : 1



File Name : Table3.ps

Title : Graphics produced by IDL

Creator : IDL Version 4.0.1 (MacOS Po

CreationDate : Fri Sep 12 16:16:24 1

Pages : 1



File Name : G96oxyg.ps
Title : Graphics produced by IDL
Creator : IDL Version 4.0.1 (MacOS Macin
CreationDate : Mon Feb 3 10:45:53 199;
Pages : 1



File Name : Lemcomp.ps
Title : Graphics produced by IDL
Creator : IDL Version 4.0.1 (MacOS Pow
CreationDate : Wed Aug 27 17:37:09
Pages : 1